ASSESSING THE ADDED-VALUE OF NEAR-TERM DECADAL CLIMATE INFORMATION FOR THE AGRICULTURAL SECTOR

BSC-ESS-2018-002

Balakrishnan Solaraju-Murali[1], Nube González-Reviriego[1], Louis-Philippe Caron[1] and Francisco J. Doblas-Reyes[1,2]

(1) Earth Sciences Department
Barcelona Supercomputing Center - Centro Nacional de Supercomputación (BSC-CNS), C/Jordi Girona, 29, 08034 Barcelona, Spain
(2) ICREA, Pg. Lluís Companys, 23, 08010 Barcelona, Spain

Barcelona, 18 October 2018

Series: Earth Sciences (ES) Technical Report

Barcelona Supercomputing Center–Centro Nacional de Supercomputación (BSC-CNS)

C/Jordi Girona, 31 | 08034 Barcelona (Spain)

Contents

1. Introduction

Agriculture has been heavily influenced by recent alterations in the frequency and severity of extreme climate events such as heat waves, heavy precipitation and droughts, and the impacts is expected to further increase due to anthropogenic climate change in the upcoming decades (Füssel et al., 2017). This indicates that effective planning of agricultural mitigation and adaptative actions to the near-term (understood as the time period from one year up to a decade ahead) climate variability and change is highly desirable.

Until recently, the only source of near-term climate change information available to the interested users for assessing the impact of climate change on the crop yield and crop productivity were climate projections (referred to as non-initialized climate simulations, in this report). These projections provide a future outlook on the evolution of the Earth's climate system, covering a continuous temporal period ranging from the past century to the end of this century (or beyond). The evolution of a climate system represented in such simulations are solely driven by prescribed changes in the atmospheric composition and other external forcings. Over the course of the last few years, initialized decadal climate predictions have been made available for users as a potential source of near-term climate information with the aim of supporting climate-related decisions in key societal sectors such as agriculture. These decadal predictions are initialized with observation-based data and then run for a decade or so under the influence of contemporaneous changing external forcings, similar to climate projections (for instance, with increasing greenhouse-gas concentration).

In this context, the study aims to explore the usage of these recent decadal predictions and illustrate the added-value of initialized predictions over non-initialized climate simulations for building a reliable climate service for agricultural needs on a multi-annual to decadal timescale. This document is organized as follows: section 2 provides the details of the dataset (both the models and observations) used and describes the specifics of the decadal forecast system simulations that are considered in this study. Section 3 describes the bias-adjustment technique applied to the decadal predictions, the steps to compute agro-climatic indices and the Pearson correlation used to assess the forecast quality of the predictions. Section 4 presents the predictive skill of the initialized decadal predictions and the added-value it holds over non-initialized simulations. This document concludes with a set of recommendations for the operationalization of these forecasts, discuss the possibility of generating a service for the agriculture sector and suggest the way forward in the context of the Coupled Model Intercomparison Project 6 (CMIP6).

2. Data

2.1. Decadal forecast data

This study uses decadal hindcasts from two different climate models that were produced as part of the Coupled Model Intercomparison Project Phase 5 (CMIP5). The two climate models considered are: EC-Earth (Hazeleger et al., 2012), which is developed by the EC-Earth consortium, counting close to 20 European institutions and the GFDL-CM2.1 (Delworth et al., 2006), which is developed by the Geophysical Fluid Dynamics Laboratory (GFDL). A summary of the CMIP5 decadal prediction experimental design can be found in Taylor et al. (2012; see also https://pcmdi.llnl.gov/mips/cmip5/).

Since the main objective of this study is to assess the skill of the climate forecast systems, only the hindcasts are chosen. Hindcasts are the reforecasts of the past, where observations are available to evaluate the forecast skill. For this study, two types of simulations are considered.

1) Near-term initialized decadal simulations (INIT): These are a set of 10-year long initialized hindcasts that were run by explicitly prescribing the contemporaneous state of the climate system at the start of the simulation (November 1 of each year from 1960 to 2011 in the case of EC-Earth; January 1 of each year from 1961 to 2012 in the case of GFDL-CM2.1), while also accounting for changes in radiative forcings (both natural and anthropogenic; prescribed with the estimates of observed changes in radiative forcing until 2005, and estimated forcing according to the RCP4.5 scenario thereafter). This experiment will be simply referred to as 'INIT' in this study.
2) Long-term historical experiments (No-INIT): These are non-initialized simulations, which do not include the details of the contemporaneous state of the climate system. These simulations are usually started from an arbitrary initial condition derived from the multi-century preindustrial control simulation and then run by forcing the observed atmospheric composition changes (reflecting both anthropogenic and natural sources) over the period 1861-2100. However, in this study, we restrain our analysis to the period corresponding to the 'INIT' simulations. These simulations use the same changes in radiative forcing as prescribed in 'INIT' simulation, and are primarily intended to estimate the forced response of the climate system. We refer to these simulations as the 'No-INIT' experiments.

EC-Earth runs both simulations at 1.25°x1.25° resolution and include 5 ensemble members whereas GFDL-CM2.1 simulations are run with a 2.5°x2.5° global grid and include 10 ensemble members. In this study, for each climate model, monthly data of temperature and precipitation for the first 5 forecast years of the INIT and No-INIT hindcasts between the period 1961-2010 over the European domain (33°N-75°N, 15°W-44°E) were considered. These two models were chosen from a larger pool of models primarily due to the availability of simulations initialized every year between 1961-2011/2012.

2.2. Reference forecast

In this study, we focus on evaluating the forecast quality of agro-climatic indices based on two-meter temperature and precipitation. For this, the reference datasets used are GHCN-CAMS Version 2 (Fan and van den Dool, 2008) for two-meter temperature and GPCC Version 7 (Schneide et al., 2016) for precipitation. GHCN-CAMS Version 2 is a gridded dataset, where the temperature data are taken from GHCN version 2 (Peterson and Vose, 1997) and CAMS (Ropelewski et al., 1984). This dataset is available on a global 0.5°x0.5° grid from 1948 to near present. GPCC Version 7 provides monthly totals of precipitation from 1901 to near present on a global 2.5°x2.5° grid. These two datasets are selected due to their temporal and geographical coverage and their spatial resolution.

In order to compare the dataset, the values of the climate variables are interpolated using conservative approach, from their original grid to a grid with 2.5° spatial resolution, as this was identified as the coarsest grid among the model and reference dataset considered here.

3. Methodology

This section provides the details on the research methodology and approach followed in this study.

3.1. Bias adjustment

The climate model data suffer from systematic errors and biases due to their inability in resolving some of the climate processes that occur at a spatial scales finer than that of the grid cells (e.g. evaporation of moisture from the Earth's surface, cloud formation and turbulence). This causes the model's climatology to be different than that of the observed reference. For this reason, it is necessary to carefully remove these biases in order to extract useful information (in terms of usability by end users) from the simulations.

In this study, the lead-time dependent biases in temperature and precipitation are adjusted using a simple mean bias-adjustment technique (as recommended by ICPO, 2011) in leave one out cross-validation (CV) mode. Figure 1 provides the steps involved in a typical leave one out cross validation technique used to compute the monthly average of temperature and precipitation climate variables. In CV mode, each variable (temperature or precipitation) is split into two parts: test year and training period. The training period is the entire period neglecting the test year. Following which, the average over the entire training period of the observed ($\underline{X}_{CV\_obs}$) and forecasted ($\underline{X}_{CV\_fsct}$, along each forecast year and member) variables (temperature 'T' or precipitation 'P') is obtained.

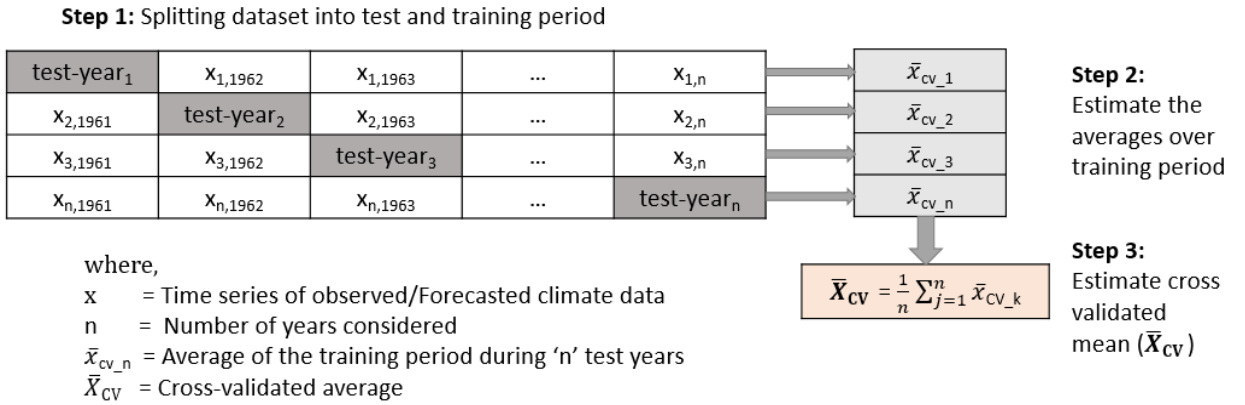

Figure 1. Schematic illustrating the step-by-step procedure of the cross validation technique applied in this study.

The cross-validated monthly averages were then used to bias-adjust the model output. For temperature, we used an additive correction along the forecast year (for all the members individually), to adjust the monthly mean values in the forecast to the observed climatological monthly mean values, as shown in equation (1).

$$T_{CV\_fsct}(j) = T(j) - (\underline{T}_{CV\_fsct} - \underline{T}_{CV\_obs}) \quad ; \text{where j = 1,..,'n' years} \qquad (1)$$

For precipitation data, a multiplicative correction is applied, as shown in equation (2).

$$P_{CV\_fsct}(j) = P(j) * (\underline{P}_{CV\_fsct} / \underline{P}_{CV\_obs}) \quad ; \text{where j = 1,..,'n' years} \qquad (2)$$

3.2. Computation of agro-climatic indices

This study considers the following three indicators: the Standardized Precipitation Evapotranspiration Index (SPEI6; Vicente-Serrano et al., 2010), the six-month mean temperature index (T6) and the six-month precipitation mean index (P6). All the above-mentioned indices are based on monthly mean temperature and total precipitation datasets.

3.2.1. Drought indicator (SPEI6)

In this work, we have assessed the skill of the climate model at forecasting drought conditions over the forecast years 2 to 5. These drought conditions are estimated using the standardized precipitation evapotranspiration index over a 6 month temporal scale (SPEI6; Vicente-Serrano et al., 2010). The process of computing the SPEI6 index can be distilled down to two steps: accumulation and standardization. First, the accumulation step involves an estimation of monthly climatic water balance ($d_{i,j}$), which provides a measure of the water surplus or deficit for a specific month 'i' in the year 'j'. It is estimated as follows:

$$d_{i,j} = (P_{i,j} - PET_{i,j}) \qquad (3)$$

where, P is the precipitation and PET is the Potential Evapotranspiration. Figure 2(a) shows the schematic of a simplified climatic water balance. In this study, we chose Thornthwaite method for estimating PET (Thornthwaite, 1948) owing to its simplicity and limited data requirements (monthly mean temperature and the latitudinal coordinates of each considered grid). Then, for each available year 'j' and each month 'i' for which SPEI6 will be estimated, the $d_{i,j}$ values are accumulated over a period of six-months. In this study, we focus on the accumulated values for the summer months June (i=6), July (i=7), August (i=8) and September (i=9) of each year. For example, $D_{6,j}$ (accumulated value for the month of June) is obtained as the sum of estimated January to June 'd' values for a specific year 'j'. The general expression for any month "i" is as follows:

$$D_{i,j} = d_{i,j} + d_{i-1,j} + .. + d_{i-5,j} \quad (4)$$

The standardization step fits the six-month accumulated $D_{i,j}$ data to a suitable parametric probability distribution and then transform the data into a standardized series (with mean = 0 and standard deviation = 1), where the standardized value is referred to the $SPEI6_{i,j}$. These two steps are carried out individually for each ensemble member and start date of the hindcast dataset. Positive values of SPEI6 corresponds to conditions of above-normal precipitation whereas negative values correspond to dry periods. Figure 2(b) illustrates the observed SPEI6 index of August for the year 2003, which was found to be one of the driest year in Europe. In this study, we use the three-parameter shifted log-logistic probability distribution function to fit the $D_{i,j}$ series, in which the parameters used to build the distribution were computed using the method of unbiased probability weighted moments (Vicente-Serrano et al., 2010). In addition to this, we have also attempted the standardization step based on the non-parametric approach (as used in Turco et al., 2017), where the accumulated $D_{i,j}$ is fitted to a standard gaussian distribution with mean 0 and standard deviation 1. No significant difference was found in the forecast quality between these two methods over Europe. Appendix I (Figure A1) compares the results obtained with the parametric and non-parametric approaches.

Since the primary goal of this study is to assess the multi-annual predictive skill of SPEI6 over the forecast years 2 to 5, two multi-annual averaging techniques were devised.

1. Applying multi-annual averaging (forecasted years 2 to 5) on the accumulated "D" data immediately after the accumulation step. In this approach, the probability distribution fitting and standardization is performed over the multi-annual averaged accumulation "D" data.
2. Applying multi-annual average after the standardization step. In this method, the $SPEI6_{i,j}$ index were averaged over the forecasted years 2 to 5.

The difference in forecast quality between these two approaches were assessed and no significant changes was found. Appendix I (Figure A2) presents the forecast quality assessment of the above-mentioned multi-averaging techniques.

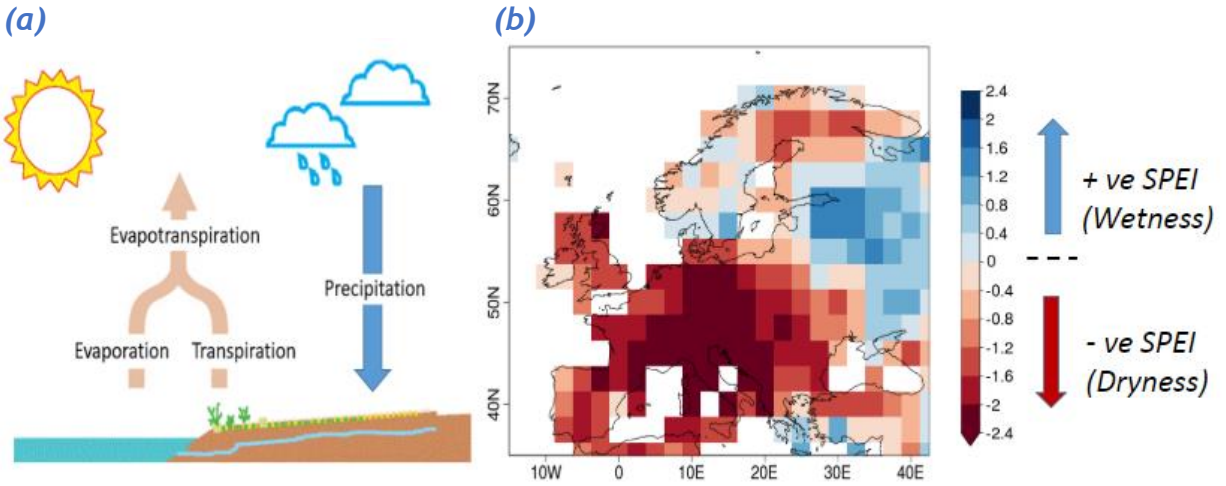

Figure 2. (a) Schematic diagram of a simplified climatic water balance (b) Observed SPEI6 for August 2003, which was an extremely dry year in Europe (extreme drought event).

3.2.2. Six-month mean temperature and precipitation indices (T6, P6)

To evaluate the SPEI6 forecast quality and the contribution of temperature and precipitation to the skill, two agro-climatic indices: six-month mean temperature (T6) and precipitation (P6), are formulated. The monthly mean temperature and precipitation values that are involved in estimation of T6 and P6 indices are combinedly used in the computation of the six-month accumulated climate water balance 'D' values (see Eq. 3 and 4).

T6 is defined as the six-month running mean of monthly temperature along the forecast time dimension. It provides an extended seasonal climate outlook of the variations in temperature. For instance, for the January 1st 1961 start date, the value of T6 for the month 6 of the first forecast year (June 1961) is the average of monthly temperatures for months 1 to 6 (i.e., January to June 1961); the value of T6 for the month 7 for the first forecast year (July 1961) is the average monthly temperatures of months 2 to 7 (February to July, 1961), and so on. The same procedure is repeated for each start date in the hindcast dataset and each ensemble member is treated independently.

Since we aim to analyze the skill of this index at the multi-annual timescale (forecasted years 2 to 5), a four-year average of the index is performed over forecast years 2 to 5 for each month, start date and ensemble member individually. For example, considering the start date January 1st 1961, the multi-annual average (forecast years 2-5) of T6 for the month of June is the average of T6 June values for the years between 1962-1965. We choose to use 4 year average, as it has been widely accepted as a compromise to potentially remove any unpredictable interannual variability present in the near-term decadal climate information (Goddard et al., 2013). This procedure is repeated for each start date and ensemble member.

The observed ($T6_{obs}$) or forecasted ($T6_{CV\_fsct}$) 6-month mean temperature index for a particular month 'i', ensemble member and start date for average years 2-5 can be obtained using the following equation:

$$(T6_{CV\_fsct})_{i,j2to5} = \frac{1}{4}\sum_{j=2}^{5} \frac{1}{6}[(T_{CV\_fsct})_{i,j} + (T_{CV\_fsct})_{i-1,j} + .. + (T_{CV\_fsct})_{i-5,j}] \quad (4)$$

$$(T6_{obs})_{i,j2to5} = \frac{1}{4}\sum_{j=2}^{5} \frac{1}{6}[(T_{obs})_{i,j} + (T_{obs})_{i-1,j} + .. + (T_{obs})_{i-5,j}] \quad (5)$$

In order to compute the six-month mean precipitation index (P6), the same methodology is followed, but we use the monthly total in precipitation instead of the monthly mean temperature.

3.3. Verification

Forecast quality assessment is considered to be a fundamental step in climate predictions. It measures how well the predicted climate variables (or the agro-climatic indices) match the verification data (observations in this case). In this report, we use the Pearson correlation coefficient (*r*) to assess the forecast quality of the SPEI6, six-month mean temperature and precipitation indices. *r* measures the linear relationship between the predicted and observed indices time series. It is important to note that the Pearson correlation is computed using the ensemble mean time series of each index along with the corresponding observational time series data. The confidence interval for *r* between a hindcast dataset and the observational reference is computed by performing a t-test, after a Fisher Z-transformation whereas the significance of correlation differences between two hindcast simulations (INIT and No-INIT) is estimated using the methodology proposed by Siegert et al. (2017).

4. Results

This section presents the forecast quality of multi-annual average (forecast years 2-5) of the agro-climatic indices over Europe and illustrates the improvement in multi-annual predictive skill by using initialized decadal prediction (INIT) over non-initialized historical simulation (No-INIT) with two forecast systems: EC-Earth and GFDL-CM2.1.

4.1. Predictive skill of drought index (SPEI6)

The ensemble-mean correlation of the SPEI6 index is shown in Figure 3. Overall, initialized decadal simulations yield positive correlation values for SPEI6 over most of the domain (INIT; first and third columns of Figure 3) for both EC-Earth and GFDL-CM2.1. In particular, significant values of correlation (95% confidence level) have been found over the Mediterranean region (Southern Europe and Northern Africa in GFDL-CM2.1 and Northern Africa in EC-Earth). The rest of Europe presents areas with non-significant positive or negative

values, which varies depending on the month and the model. GFDL-CM2.1 shows slightly better skill than EC-Earth, which could be partly linked to the difference in number of ensemble members between the two forecast systems (10 in the case of GFDL-CM2.1; 5 for EC-Earth).

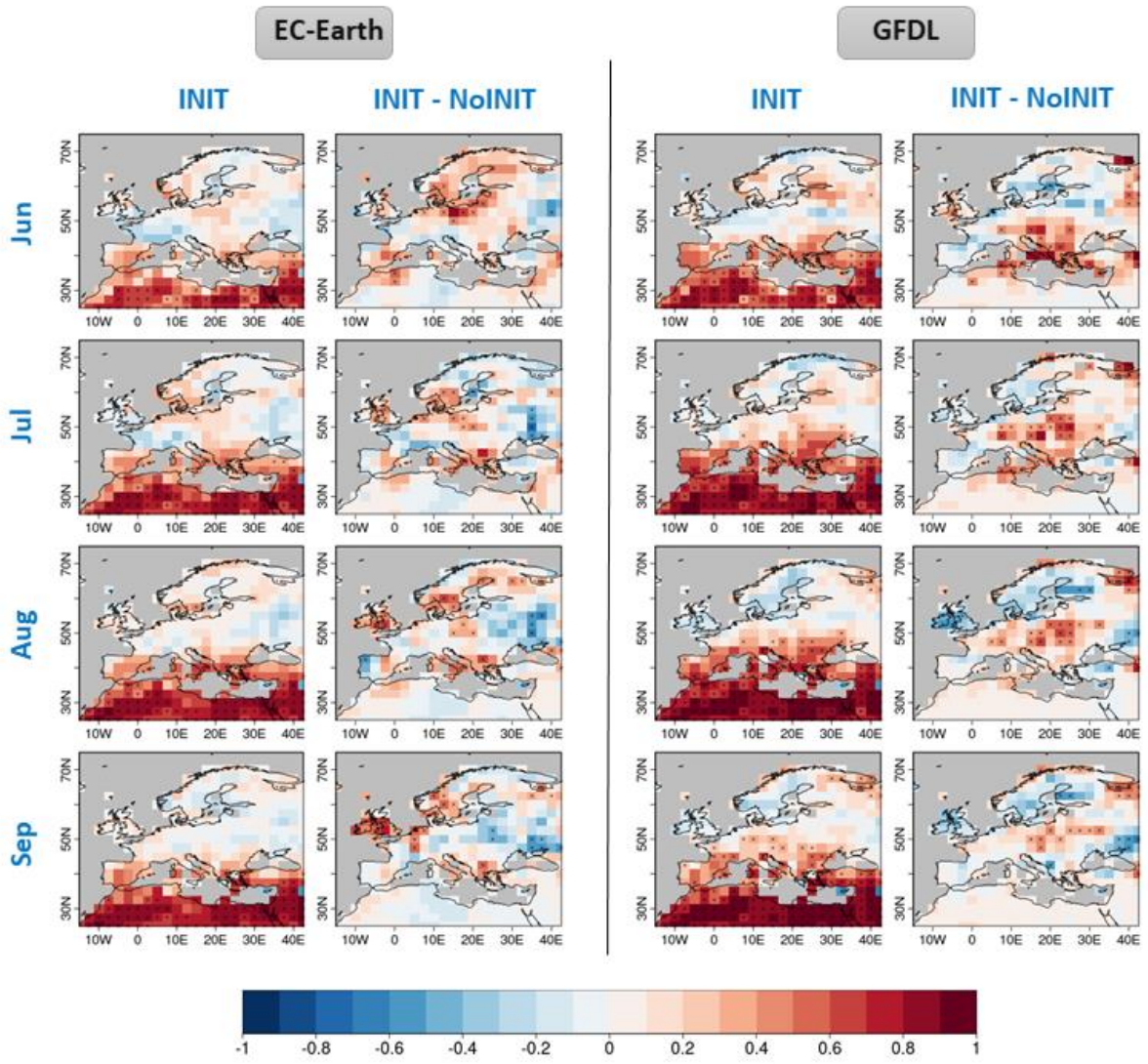

***Figure 3**. Ensemble-mean correlation coefficients of the SPEI6 index for the summer months (June to September) averaged over forecast years 2 to 5. The first and third columns corresponds to the correlation of the initialized decadal simulations (INIT) while the second and fourth columns show the difference in correlation between initialized and non-initialized climate simulations (INIT-NoINIT) performed with the EC-Earth (left) and GFDL-CM2.1 (right) decadal forecast systems. Dotted grids represent values statistically significant at 95% confidence level for SPEI6.*

The second and fourth columns of Figure 3 show the difference in correlation between initialized decadal simulations and non-initialized simulations (INIT-NoINIT). GFDL-CM2.1 shows significant improvement (dotted red coloured areas) over most of Central Europe and the Balkan region in all four summer months considered whereas EC-Earth has improved skill over Northern Central Europe from June to August.

Results of the ensemble mean correlation values for SPEI6 index obtained for the remaining months of the year can be found in the Appendix II (Figure A3-A4). These maps have been estimated in order to find a window of opportunity in skillfully predicting the extreme drought or extreme wet period.

4.2. Predictive skill of six-month mean temperature and precipitation (T6, P6)

Figure 4 displays the ensemble mean correlation of six-month mean temperature index (T6) averaged over the forecast years 2 to 5 for the summer months (June, July, August and September). For both EC-Earth and GFDL-CM2.1, initialized decadal simulations show statistically significant positive correlation values (95% confidence level) over most of the region considered (INIT; first and third columns of Figure 4).

The second and fourth columns of Figure 4, which present the correlation difference between the initialized decadal simulations and the non-initialized simulations (INIT-NoINIT), show that initializing the decadal forecast system has improved the T6 predictive skill for the months of June and July over most part of Europe with both EC-Earth and GFDL-CM2.1. However, the differences are not statistically significant. For the months of August and September EC-Earth displays non-significant negative correlation values over Europe whereas GFDL presents non-significant positive correlation values over Central and Northern Europe during the same period.

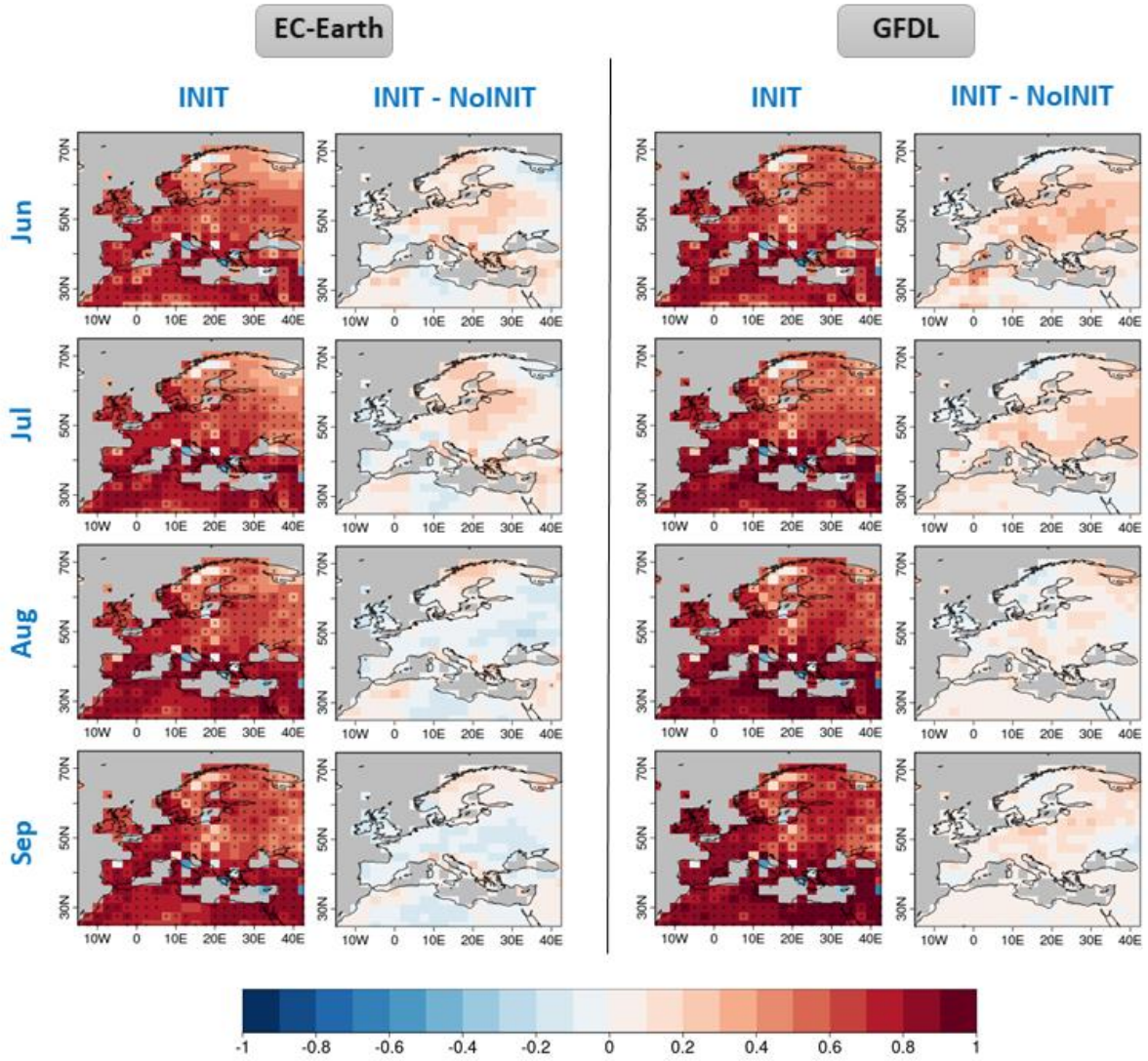

***Figure 4**. Same as Figure 3 but for the six-month mean temperature index T6. The hindcasts are verified against GHCN-CAMS version 2 dataset.*

Figure 5 presents the ensemble mean correlation of six-month mean precipitation index (P6) averaged over the forecast years 2-5 for the four summer months (June, July, August and September). In comparison to T6, the correlation values for P6 are relatively lower over most parts of the domain. GFDL-CM2.1 shows higher and significant positive correlation values over Southern Europe, Central Europe and Scandinavia for most of the same 4 months. EC-Earth shows similar spatial patterns of correlation but with a smaller fraction of significant values and larger areas of negative correlations, in particular over Southern Europe.

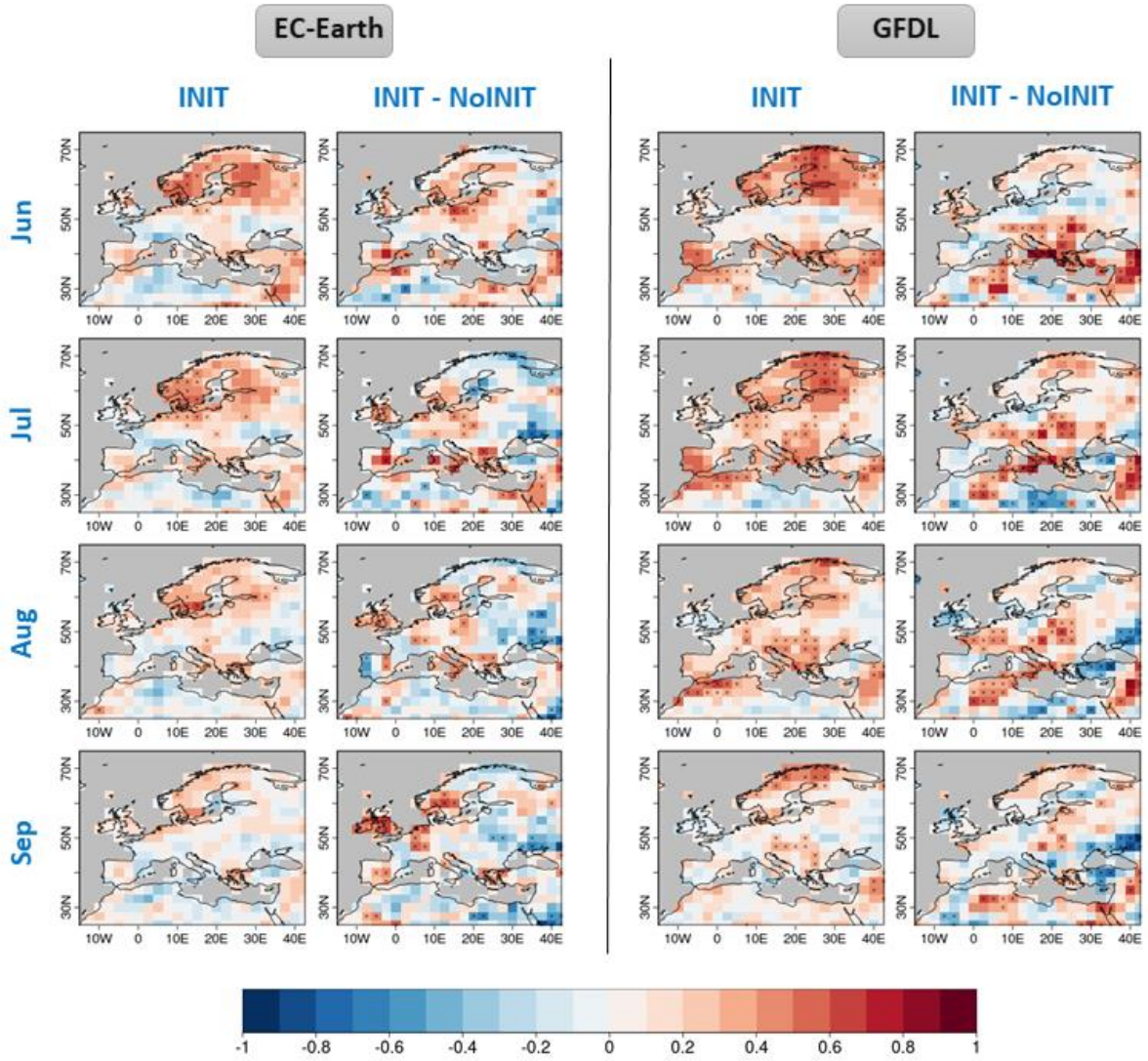

***Figure 5**. Same as figure 3 but for the six-month precipitation average index P6. The hindcasts are verified against GPCC version 7.*

The second and fourth columns of Figure 5 display differences between correlation values obtained with the INIT and No-INIT simulations. For most months, EC-Earth exhibits positive and significant differences over Northern Central Europe whereas GFDL-CM2.1 shows positive and significant differences over Southern Europe, Eastern Central Europe and the Balkan region. In addition, non-significant positive values are consistently found over UK with EC-Earth and over Scandinavia with GFDL-CM2.1.

By comparing the forecast quality of agro-climatic indices (SPEI6, T6 and P6) obtained with initialized decadal simulations (i.e., the first and third columns of Figures 3-5), we can evaluate the contribution of temperature and precipitation to the SPEI6 skill. It is evident

from this comparison that the high predictive skill of six-month mean temperature (and partly, precipitation) has significantly contributed to the positive skill in forecasting SPEI6 over the Mediterranean region (Southern Europe and Northern Africa). From the second and fourth columns of Figure 3-5, the spatial pattern of correlation difference between six-month mean precipitation index and SPEI6 indicates that the observed improvement in precipitation skill in initialized decadal simulations with respect to non-initialized simulations is primarily responsible for the enhancement in SPEI6 predictive skill.

This analysis of both T6 and P6 has been further extended for the remaining months of the year in Annex II (Figure A5-A8).

5. Conclusion

In this study, we have assessed the forecast quality of initialized decadal climate predictions for the summer months (June, July, August and September) over Europe of agro-climatic indices (SPEI6, T6 and P6). In all the cases, we have compared the initialized experiments with the non-initialized simulations in order to show the added-value of initialization. The results show reasonable skill in predicting the multi-annual averages of these agro-climatic indices over most of the studied region with both EC-Earth and GFDL-CM2.1. We also showed that initialized decadal simulations have improved the predictive skill with respect to the non-initialized simulations across various European regions during the summer months. In particular, a significant improvement in predictive skill of SPEI6 and P6 are found over the Northern Central Europe with EC-Earth and GFDL has improved predictive skill over Central Europe, Balkan region.

This study is the first of its kind because decadal climate prediction has only been recently considered for specific applications, but the encouraging results found suggest further analyses. For instance, a multi-model study would provide an idea of the robustness of the positive impact of the initialization of the simulations. At the same time, combining the predictions from all the individual systems into a single source of information might provide a more reliable and skilful forecast, as it has already been shown for climate predictions at other time scales. Such a multi-model exercise will be based on the simulations produced by the contribution of the Decadal Climate Prediction Project to the Sixth Phase of the Coupled Model Intercomparison Project (CMIP6). In this contribution, more than ten institutions will perform decadal prediction experiments with at least ten members and with up to five forecast years initialized once a year over the period 1960 to 2015. They will also provide actual forecasts for the period 2016 to 2020.

Beyond 2020, the access to decadal climate predictions will be ensured by the initiative set by the World Meteorological Organisation (WMO) to establish global producing centres, mimicking what was established more than a decade ago for seasonal climate prediction. This

initiative is being developed as part of the World Climate Research Programme Grand Challenge on Near-Term Climate Prediction, which is creating the exchange infrastructure and standards for the future global producing centres to share their forecasts with the lead centre at the Met Office. In preparation, the BSC has already been recognized by WMO as one of the four existing global producing centres. An important aspect of this evolution of decadal climate prediction is the access to the real-time forecasts, which at this stage has been defined as only available to meteorological services and public agencies working closely with them. The BSC is committed to keep working with representatives of the public and private sector to illustrate the benefits of decadal climate prediction and is ready to share its forecasts and the multi-model gathered by the lead centre under collaboration agreements.

Much more research and development is still missing to improve decadal climate prediction systems. Adequate solutions for the problems of the multi-model combination, forecast post-processing, merging of both dynamical and empirical systems into a single source of information, robust forecast quality assessment, downscaling, etc. are required. And this is without mentioning the need to reduce systematic model errors and improving the forecast initialization.

References

Delworth, T. L., Broccoli, A. J., Rosati, A., Stouffer, R. J., Balaji, V., Beesley, J. A., & Coauthors. (2006). GFDL's CM2 global coupled climate models. Part I: Formulation and simulation characteristics. Journal of Climate, 19(5), 643-674, doi: 10.1175/JCLI3629.1.

Fan, Y., & Van den Dool, H. (2008). A global monthly land surface air temperature analysis for 1948–present. Journal of Geophysical Research: Atmospheres, 113(D1), doi: 10.1029/2007JD008470.

Füssel, H. M., Jol, A., Marx, A., Hildén, M., Aparicio, A., Bastrup-Birk, A., & Coauthors. (2017). Climate change, impacts and vulnerability in Europe 2016-An indicator-based report, EEA Report, Vol. 1/2017, doi:10.2800/534806

Goddard, L., Kumar, A., Solomon, A., Smith, D., Boer, G., Gonzalez, P., & Coauthors. (2013). A verification framework for interannual-to-decadal predictions experiments. Climate Dynamics, 40, 245-272, doi:10.1007/s00382-012-1481-2.

Hazeleger, W., Wang, X., Severijns, C., Ştefănescu, S., Bintanja, R., Sterl, A., & Coauthors. (2012). EC-Earth V2. 2: description and validation of a new seamless earth system prediction model. Climate dynamics, 39(11), 2611-2629, doi: 10.1007/s00382-011-1228-5.

ICPO - International CLIVAR Project Office. (2011). Data and bias correction for decadal climate predictions. International CLIVAR Project Office, CLIVAR Publication Series 150, 6pp Available at https://eprints.soton.ac.uk/171975/1/ICPO150_Bias.pdf

Peterson, T. C., & Vose, R. S. (1997). An overview of the Global Historical Climatology Network temperature database. Bulletin of the American Meteorological Society, 78(12), 2837-2850, doi: 10.1175/1520-0477(1997)078<2837:AOOTGH>2.0.CO;2.

Ropelewski, C. F., Janowiak, J. E., & Halpert, M. S. (1984). The Climate Anomaly Monitoring System (CAMS), Climate Analysis Center, NWS, NOAA, Washington DC, 39pp, Available from the Climate Prediction Center, Camp Springs, MD 20746.

Schneider, U., Becker, A., Finger, P., Meyer-Christoffer, A., Rudolf, B., & Ziese, B. (2016). GPCC full data reanalysis version 7.0: monthly land-surface precipitation from rain gauges built on GTS based and historic data. Research data archive at the National Center for Atmospheric Research, Computational and Information Systems Laboratory, doi: 10.5065/D6000072.

Siegert, S., Bellprat, O., Ménégoz, M., Stephenson, D. B., & Doblas-Reyes, F. J. (2017). Detecting improvements in forecast correlation skill: Statistical testing and power analysis.

Monthly Weather Review, 145(2), 437-450, doi: 10.1175/MWR-D-16-0037.1.

Thornthwaite, C. W. (1948). An approach toward a rational classification of climate. Geographical review, 38(1), 55-94, doi: 10.2307/210739.

Turco, M., Ceglar, A., Prodhomme, C., Soret, A., Toreti, A., & Francisco, J. D. R. (2017). Summer drought predictability over Europe: empirical versus dynamical forecasts. Environmental Research Letters, 12(8), 084006, doi: 10.1088/1748-9326/aa7859.

Taylor, K. E., Stouffer, R. J., & Meehl, G. A. (2012). An overview of CMIP5 and the experiment design. Bulletin of the American Meteorological Society, 93(4), 485-498, doi: 10.1175/BAMS-D-11-00094.1.

Vicente-Serrano, S. M., Beguería, S., & López-Moreno, J. I. (2010). A multiscalar drought index sensitive to global warming: the standardized precipitation evapotranspiration index. Journal of Climate, 23, 1696-1718, doi:10.1175/2009JCLI2909.1.

Appendix I

(i) Parametric Vs Non-parametric approach for standardizing the six-month accumulated climate balance 'D' values.

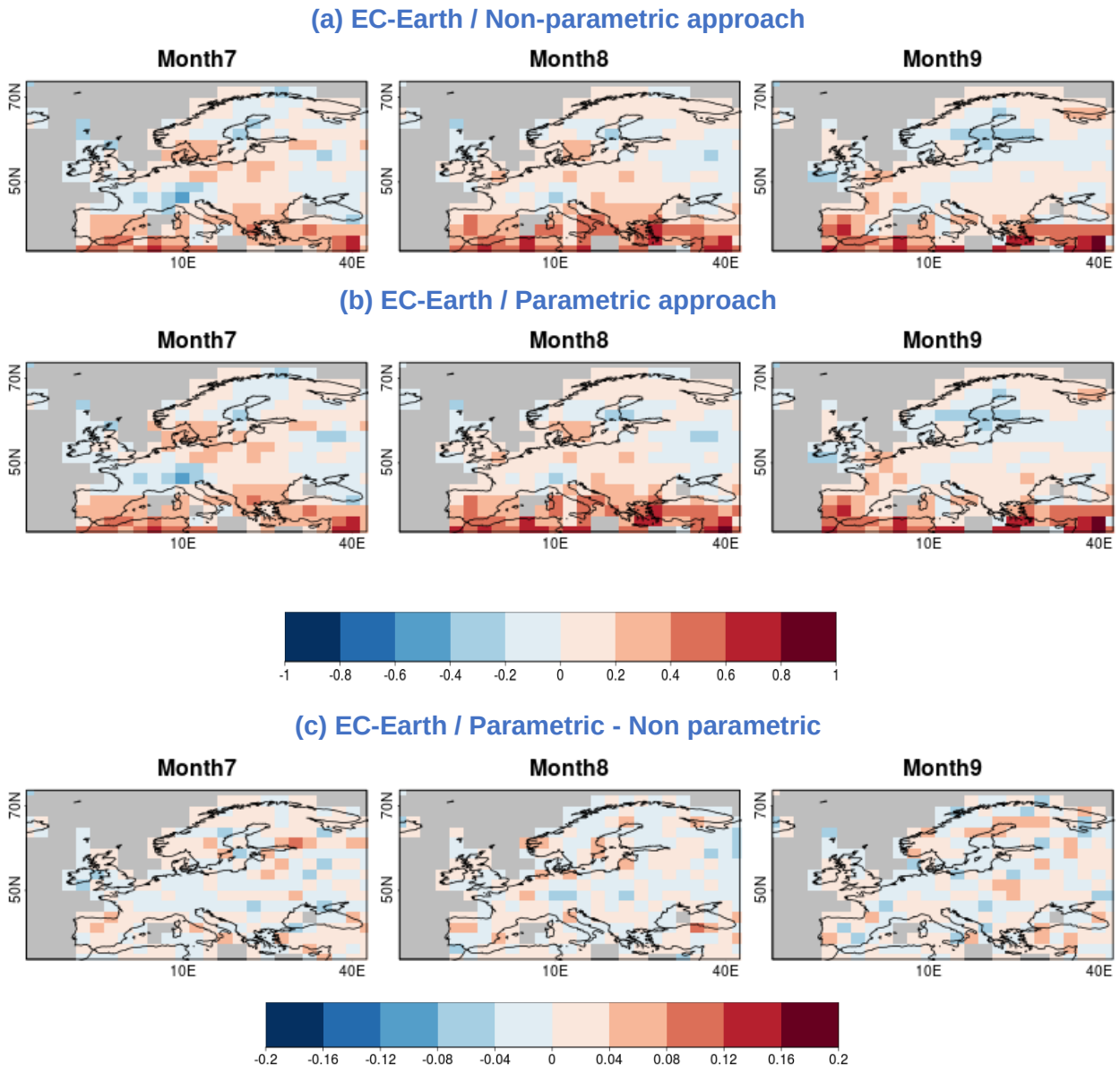

Figure A1. *Ensemble-mean correlation coefficients of the initialized decadal simulations (INIT; performed with EC-Earth decadal forecast system) for the SPEI6 index for the summer months (July to September) averaged over forecast years 2 to 5 . SPEI6 standardization based on (a) non-parametric approach (b) parametric approach (c) difference between parametric and non-parametric approach.*

(ii) Performing multi-annual averaging (forecast years 2 to 5) before and after standardization step.

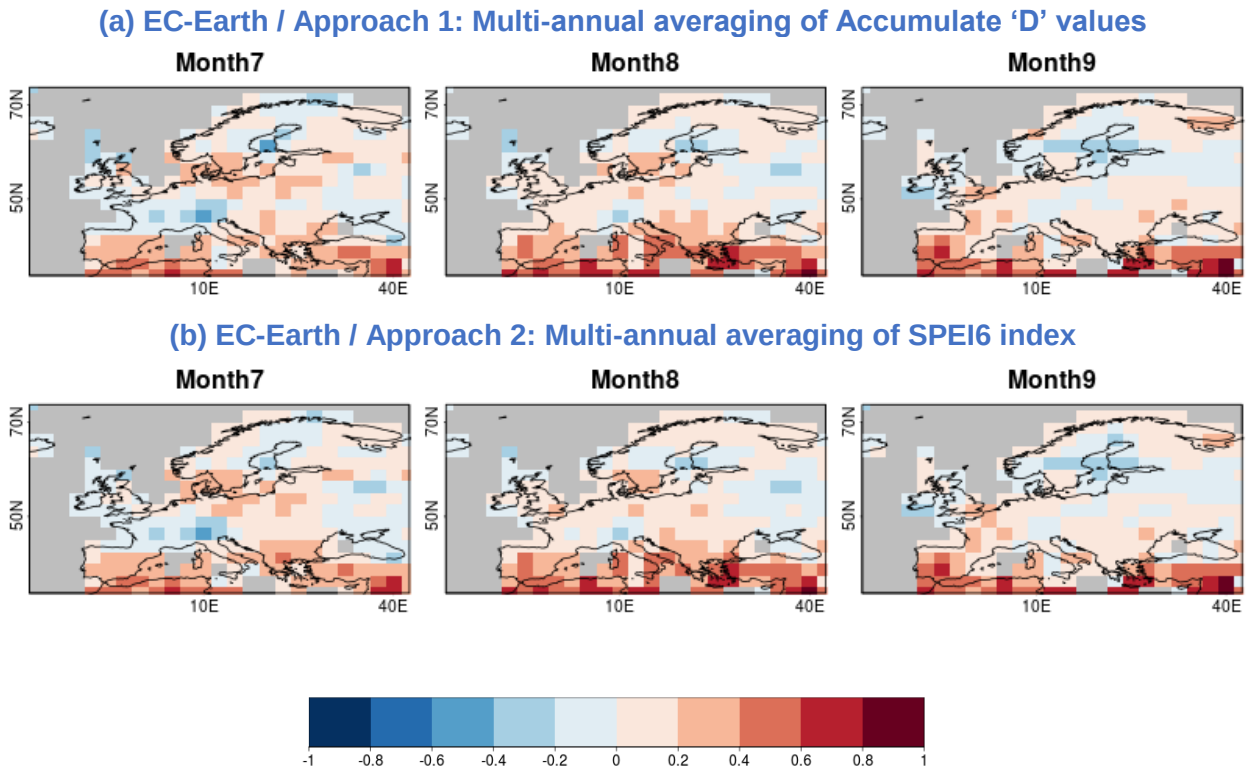

***Figure A2**. Ensemble-mean correlation coefficients for the initialized decadal simulations (INIT; performed with EC-Earth decadal forecast system) for the SPEI6 index for the summer months (July to September) averaged over forecast years 2 to 5. Multi-annual average technique applied on (a) the accumulated climate balance 'D' values (b) the computed SPEI6 index.*

Summary:

The result presented in *Appendix I* aim to illustrate that no noticeable changes are observed by using an ensemble mean correlation coefficient (as a verification measure) derived from either (a) the parametric and non-parametric approach, or (b) by performing the multi-annual averaging immediately after the accumulation step or by performing the multi-annual averaging with the computed SPEI6 index, i.e., after the standardization step. Note that this analysis was performed using a different number of members and slightly different start dates and as such are not directly commensurable with the results presented in the main part of the report.

Appendix II

Predictive skill of SPEI6

(a) INIT *(b) INIT - NoINIT*

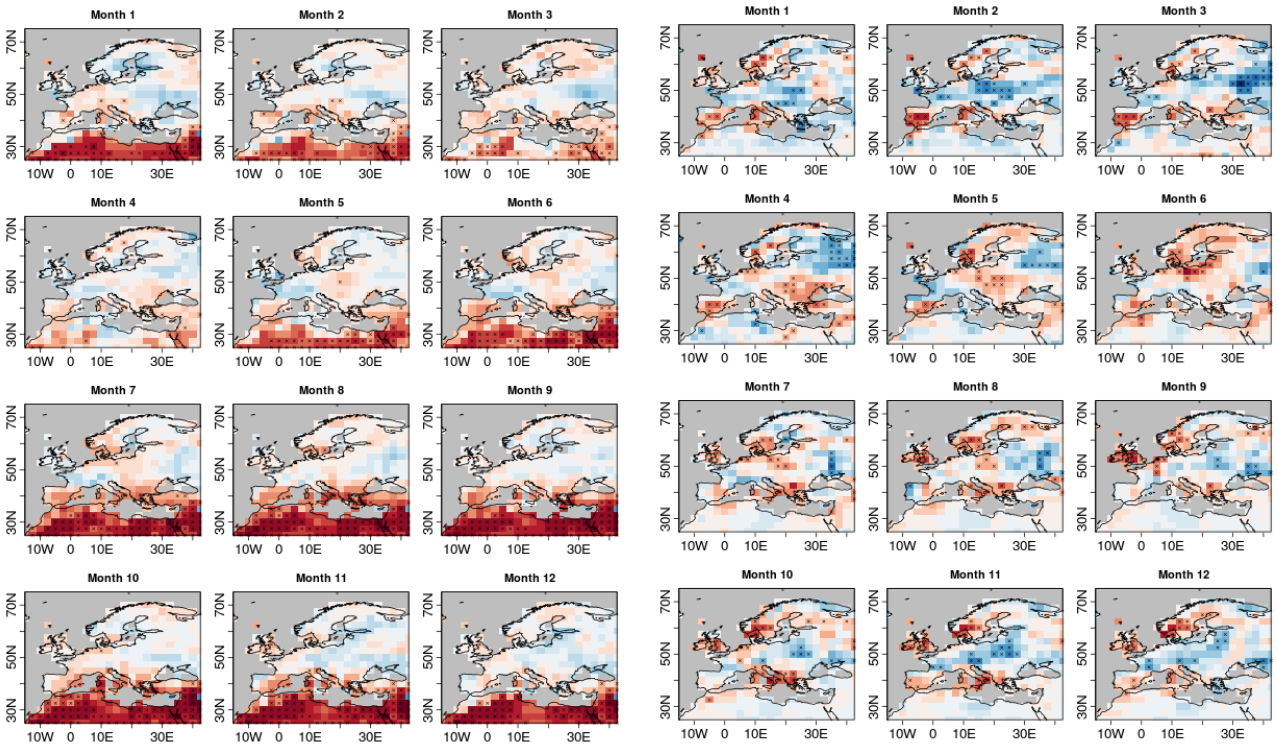

***Figure A3**. Same as figure 3, but for all the months of the year. (a) the correlation of the initialized decadal simulations (INIT) (b) the difference in correlation between initialized and non-initialized climate simulations (INIT-NoINIT) performed with EC-Earth*

(a) INIT *(b) INIT - NoINIT*

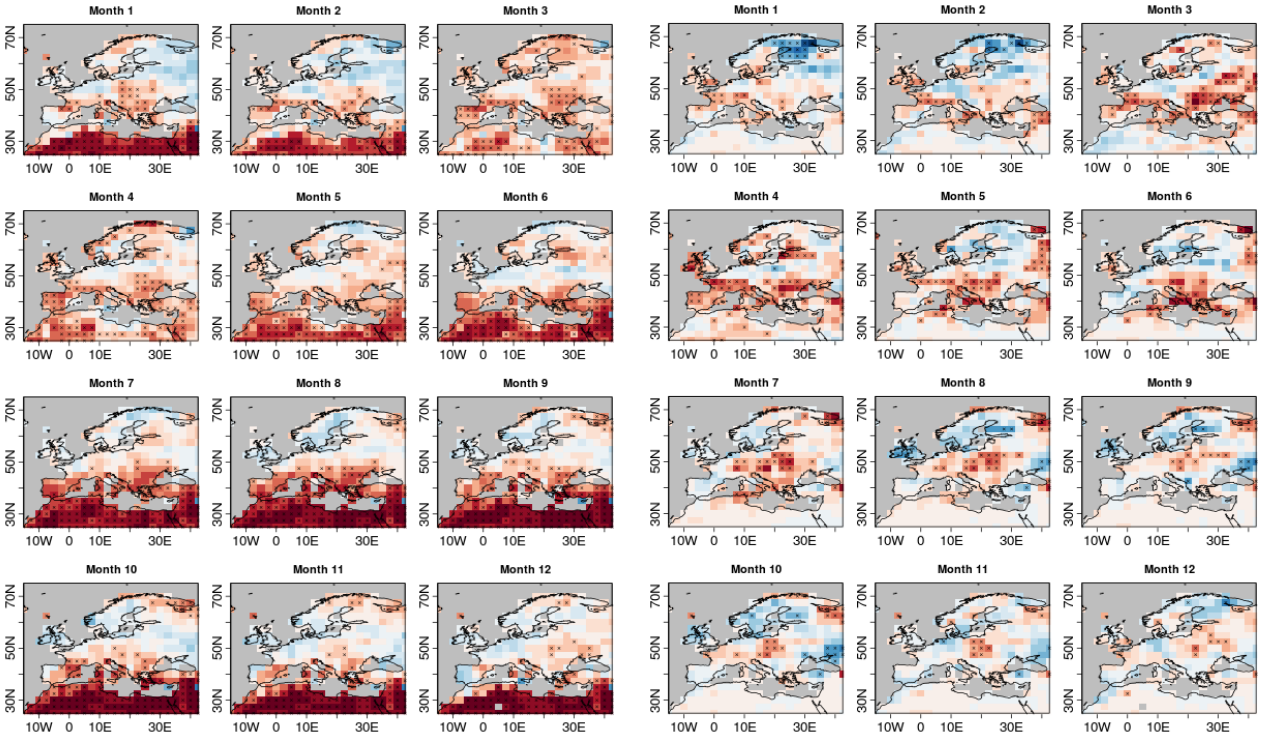

***Figure A4**. Same as figure 3, but for all the months of the year. (a) the correlation of the initialized decadal simulations (INIT) (b) the difference in correlation between initialized and non-initialized climate simulations (INIT-NoINIT) performed with GFDL-CM2.1.*

Predictive skill of six-month mean temperature index (T6)

(a) INIT *(b) INIT - NoINIT*

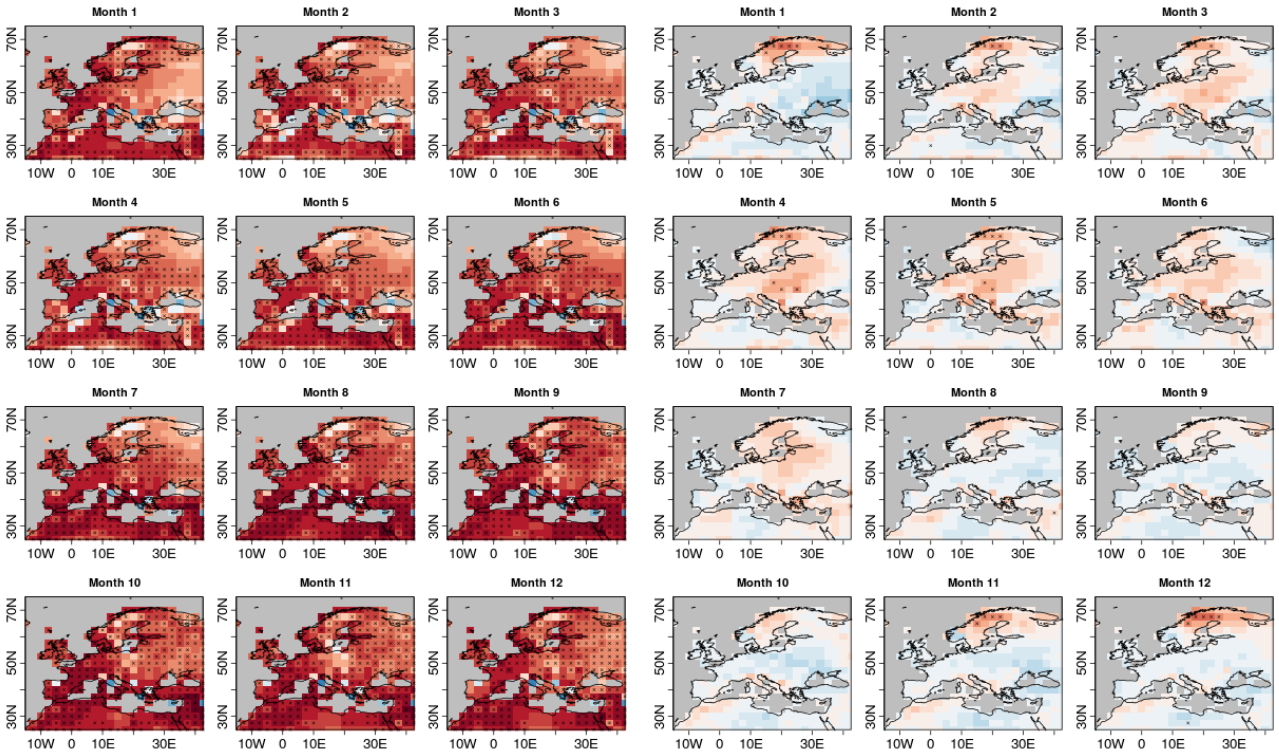

***Figure A5**. Same as figure 4, but for all the months of the year. (a) the correlation of the initialized decadal simulations (INIT) (b) the difference in correlation between initialized and non-initialized climate simulations (INIT-NoINIT) performed with EC-Earth*

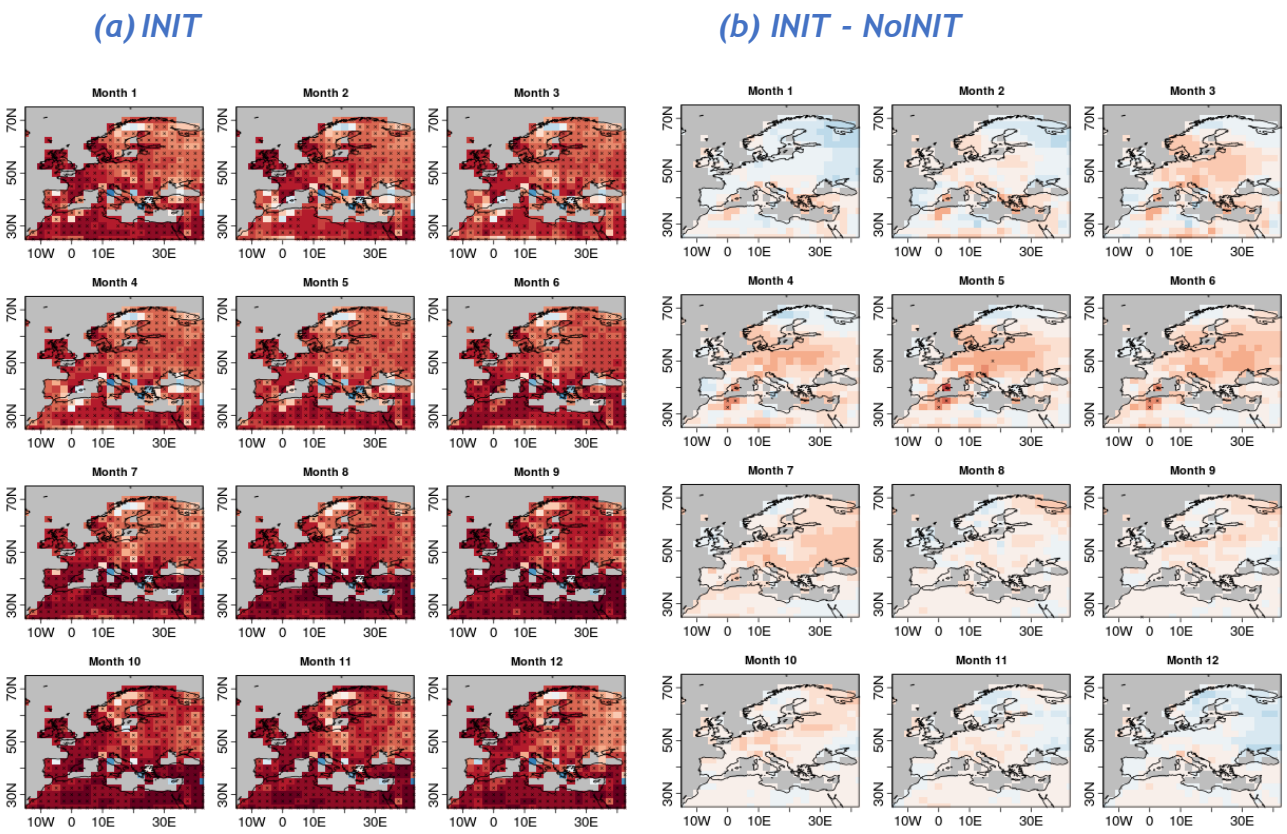

***Figure A6**. Same as figure 4, but for all the months of the year. (a) the correlation of the initialized decadal simulations (INIT) (b) the difference in correlation between initialized and non-initialized climate simulations (INIT-NoINIT) performed with GFDL-CM2.1.*

Predictive skill of six-month mean precipitation index (P6)

(a) INIT *(b) INIT - NoINIT*

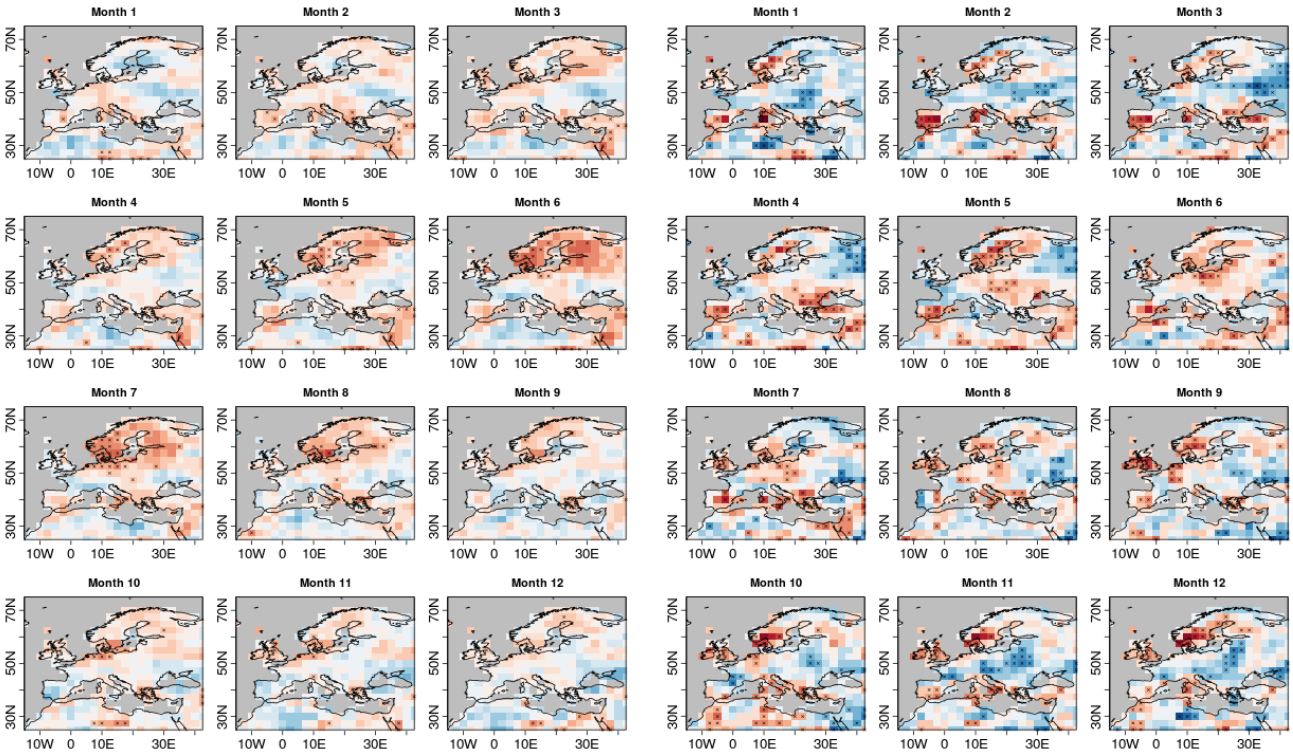

Figure A7. *Same as figure 5, but for all the months of the year. (a) the correlation of the initialized decadal simulations (INIT) (b) the difference in correlation between initialized and non-initialized climate simulations (INIT-NoINIT) performed with EC-Earth*

(a) INIT *(b) INIT - NoINIT*

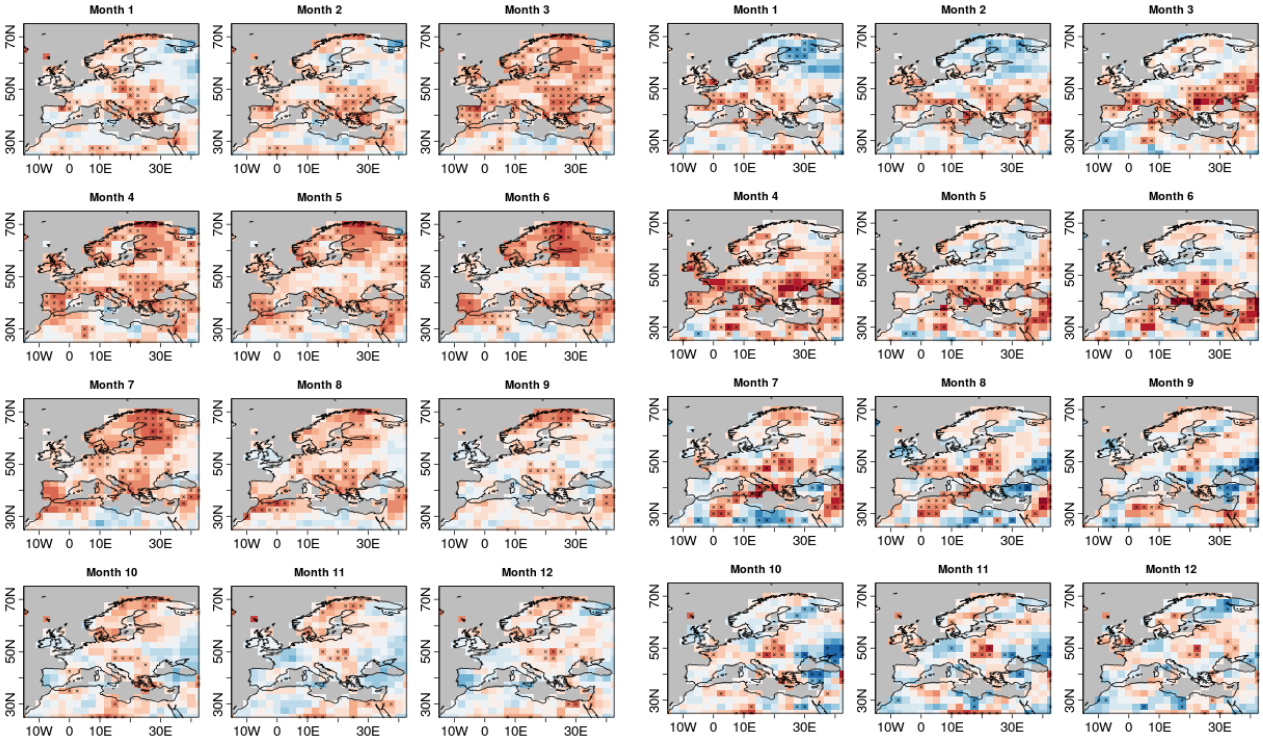

***Figure A8**. Same as figure 5, but for all the months of the year. (a) the correlation of the initialized decadal simulations (INIT) (b) the difference in correlation between initialized and non-initialized climate simulations (INIT-NoINIT) performed with GFDL-CM2.1.*